

Computation and Validation of Parameter Effects on Lobed Mixer-Ejector Performances

ZHANG Jingzhou, SHAN Yong, LI Lirguo

(College of Energy and Power Engineering, Nanjing University of Aeronautics and Astronautics, Nanjing 210016, China)

Abstract: Three-dimensional numerical computation of the flow fields and pumping performances for the lobed mixer-ejector are conducted using full Navier-Stokes equations. In the computation, the inlet of the primary flow uses the mass flowrate boundary condition. The inlet of the second flow and the outlet of the mixing flow use the pressure boundary condition. Compared with the relative experimental results, it is shown that the present calculation is reasonable. And a series of numerical studies is performed to obtain the effects of area ratio and length to diameter ratio of mixing duct on pumping coefficient and thermal mixing efficiency of a lobed mixer-ejector.

Key words: lobed nozzle; ejector; mixer; numerical computation

波瓣引射—混合器特性参数影响的数值研究和验证. 张靖周, 单勇, 李立国. 中国航空学报(英文版), 2005, 18(3): 193–198.

摘要: 运用不可压缩流动 Navier-Stokes 方程, 对波瓣喷管引射混合器的流场和引射特性进行了三维数值研究. 在计算过程中, 主流进口采用质量流量边界条件, 二次流进口和混合流出口采用压力边界条件, 均设置为环境大气压力. 与相关的实验结果对比表明本文的计算方法可以有效地预测引射流量比和混合流场. 针对混合管的结构参数开展了系列研究, 获得了混合管截面比和长径比对于引射系数和热混合效率的影响趋势.

关键词: 波瓣喷管; 引射器; 混合器; 数值计算

文章编号: 1000-9361(2005)03-0193-06

中图分类号: V231.1; V231.2

文献标识码: A

The mixer-ejector is an efficient fluid dynamic device consisting of a high velocity primary jet issuing from a nozzle into a mixing duct that is open at both ends. When the primary jet mixes out to fill the larger area cross-section of the mixing duct, the turbulent shear layer entrains a secondary flow. As a result of this mechanism, the ejector-mixers are widely used in aero-engine exhaust system for jet noise reduction, thrust augmentation, infrared radiation, Suppression and so on^[1-3]. Mixer-ejector performances are typically expressed as the ratio of the secondary to primary mass flow rate Φ and the mixing efficiency or mixing uniformity.

A relatively large number of experimental and analytical studies, which capture the fundamental aerodynamic phenomena of the lobed mixer-ejector nozzle, have been performed^[4-11]. The mixer-ejec-

tor nozzles are designed to entrain large amounts of secondary flow through an array of lobed chutes with convoluted trailing edge that are deployed into the primary stream. These lobed chutes alternating misalignment cause streamwise vortices which rapidly mix the primary and secondary flow together. The rapid internal mixing of the two streams lowers the static pressure at the nozzle exit and results in pumping capacity augmentation.

However, the knowledge about the effects of design parameters and geometric configuration on the mixer-ejector performances are not enough by now. Furthermore, the attempt to seek a reasonable method for predicting the pumping capacity of the mixer-ejector is also important. For this reason, analytical design tool is a key aspect to the successful design process, which not only saves ex-

Received date: 2004-03-26; Revision received date: 2005-03-30

Foundation item: Aeronautical Science Foundation of China

© 1994-2010 China Academic Journal Electronic Publishing House. Open access under [CC BY-NC-ND license](http://creativecommons.org/licenses/by-nc-nd/4.0/). <http://www.cnki.net>

pensive and time-consuming by test compared to CFD analysis, but also is helpful to obtain detailed insight of the flow physics in the mixer-ejector nozzle solely from test data.

To the authors' s knowledge, the numerical simulation of mixer-ejector pumping capacity is a challenging problem for the reason that the secondary flow is driven solely by the primary entrainment. In the early time, the pumping capacity prediction is based on 1-D mixing analysis^[12] in which conservation of mass flow rate, momentum, and energy are enforced. This method may predict the ideal limit for giving no consideration on the effects of the wall friction and non-uniformity of the mixing process. Zhang and Shan^[13] made an improvement by using 1-D ejector pumping relationship and full Navier-Stokes equations. Firstly, the ideal pumping coefficient was determined based on the 1-D ejector pumping relationship. Then the coefficients in the 1-D ejector pumping relationship were corrected according to the velocity distribution and wall friction resulting from the calculation of Navier-Stokes equations. So the final pumping coefficient was obtained by repeating the above process until the residual was satisfied. From the comparison between the computation results and experimental data, it was concluded that this method is reasonable in predicting the mixer-ejector pumping capacity.

The objective of this paper is to present a numerical computation and validation of pumping and mixing characteristics for lobed mixer-ejector based on Fluent-CFD software with the use of full Navier-Stokes equations and two-equation turbulence model. Especially it focuses on the research of boundary condition assignments at the inlet and outlet plane, to seek the reasonable treatment for determining the mixer-ejector pumping capacity. And a series of mixing duct parameters are varied, such as the diameter and length, to obtain better insight into the influences of mixing duct parameters on lobed mixer-ejector performance and compared with experimental data.

1 Experimental Description

The mixer-ejector test facility is shown schematically in Fig. 1. The primary flow is high pressure cold air supplied by the air compressor. It flows through a duct with diameter 80 mm. After being heated by the combustor, the primary stream with high velocity and temperature enters the lobed nozzle. The lobed nozzle has 12 lobes distributed uniformly in circumferential direction (Fig. 2). The lobe height $h = 28$ mm, lobe width $b = 7.2$ mm with the sides being parallel to each other, lobe length $l_b = 80$ mm with the expand angle of the lobe is 20° . The secondary stream is entrained to a larger chamber through two ducts having standard bell-mouth inlet located up and down of the chamber. The two flows mix in the mixing duct with constant area section and then exhaust to the ambient.

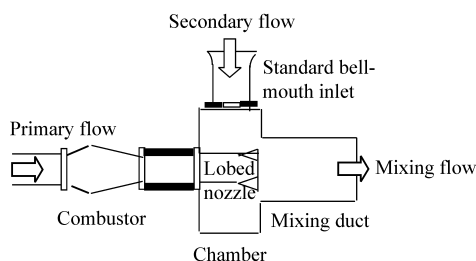


Fig. 1 Schematic of test facility

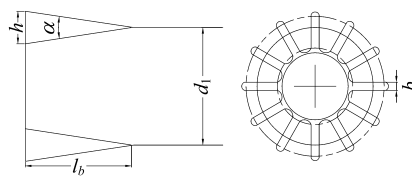


Fig. 2 Simplified mixer ejector configuration

The primary mass flowrate m_p is measured by a standard orifice plate flowmeter located in the primary air supply pipe upstream of the combustor. The primary total pressure and temperature are measured by pressure and temperature probes respectively. The secondary mass flowrate m_s is determined by static pressure in the standard bell-mouth inlet.

The temperatures of mixing flow at mixing duct exit are measured by temperature probes. And the static pressure holes on the mixing duct wall are aligned in two lines corresponding to lobe peak and

lobe trough in circumference respectively.

In the present work, the parameters of lobed nozzle are constant, a series mixing duct parameters are varied by changing the diameter and length of the mixing duct.

Numerical Procedure

2.1 Computation region

As the experimental model is axial symmetric, only half of the physical model is chosen as computational region(Fig. 3). The unstructure grids are used in the present computation and refine grids are placed near the solid wall. From CFD test it is appeared that 417 249 grid points are adequate for solving the mixing-related features of the flow field, as well as determining the pumping characteristics of the mixer ejector.

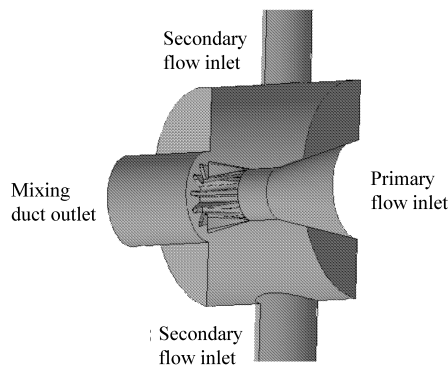


Fig.3 Schematic of computation model

2.2 Boundary conditions

The governing equation in general form is

$$\frac{\partial}{\partial x}(\rho u \phi) + \frac{1}{r} \frac{\partial}{\partial r}(r \rho v \phi) + \frac{1}{r} \frac{\partial}{\partial \theta}(\rho w \phi) = \frac{\partial}{\partial x} \left(\Gamma \frac{\partial \phi}{\partial x} \right) + \frac{1}{r} \frac{\partial}{\partial r} \left(\Gamma r \frac{\partial \phi}{\partial r} \right) + \frac{1}{r} \frac{\partial}{\partial \theta} \left(\Gamma \frac{\partial \phi}{\partial \theta} \right) + S \tag{1}$$

The turbulent viscosity is defined as

$$\eta_t = c_{\mu} \mu \rho k^2 / \varepsilon \tag{2}$$

The coefficients in the above equations are determined by RNG *k*– ε model^[14].

The boundary conditions required for the mixer ejector calculation are the mass flowrate and temperature of the primary, ambient pressure and temperature.

Flow rate boundary type is used at the primary flow inlet, with the mass flux 0. 108 kg/s and tem-

perature 620 K.

Pressure boundary types are used at the secondary flow inlet and mixing flow outlet, with pressure 101 325 Pa and temperature 300 K. The derivations of all the variables along streamwise direction are set as zero.

The velocities at the wall are set as zero and the adiabatic wall condition is applied to the energy equation. The wall law is used to treat *k* and ε near the wall.

Symmetry boundary condition is employed at the central plane.

The convergence degree for velocities, *k* and ε is chosen as 10^{–4}, for temperature is 10^{–6}.

Results and Discussion

3.1 Comparison of computation and experiment

A comparison of the calculated and measured temperature radial distributions^[10] at the mixing duct exit for the case of the area ratio $\lambda= 3.3$ (λ is defined as the area ration of mixing duct area to nozzle area) and the length to diameter ratio *L/D*= 1 is shown in Fig. 4. The temperatures are the average values in radial direction among the fan section from lobe peak to lobe trough. This comparison demonstrates reasonably good agreement between the computed and measured results, which indicates that the computational procedure in the present work is reliable to simulate the mixing flow fields.

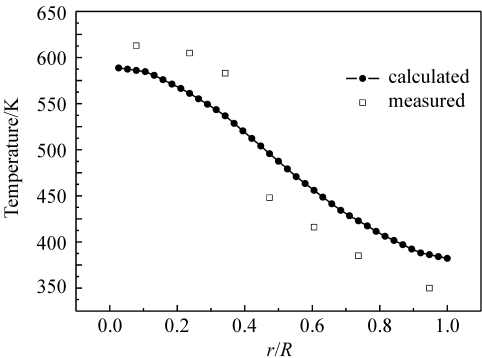


Fig.4 Comparison of calculated and measured temperature radial distributions

The comparison of the measured and calculated mixing duct static pressure distributions in the case of $\lambda= 3.3$ and *L/D*= 1 is shown in Fig. 5.

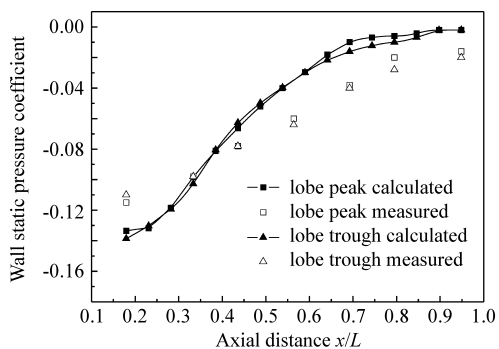


Fig.5 Static pressure distributions on mixing duct

The pressure coefficient define as

$$C_p = (p - p_{atm}) / (0.5 \rho u_p^2) \quad (3)$$

It is found that there are good agreements between the measured and calculated values in the lobe peak or trough section. The static pressure near the nozzle exit is lower and then increases gradually to ambient pressure.

Fig. 6 shows the comparison of the calculated and measured pumping ratio for different area ratios of mixing duct.

$$\Phi = m_s / m_p \quad (4)$$

here m_s is the secondary massflow and m_p is the main massflow.

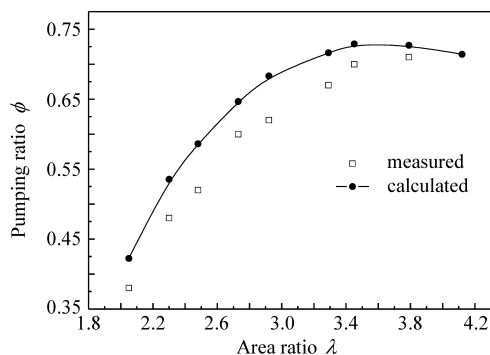


Fig. 6 The relationship of pumping ratio vs area ratio

From the comparison, it is seen that the calculated values are some greater than the corresponding experimental values and the tendency for $\Phi \lambda$ is the same. The maximum relative disagreement is about 20% in the little area ratios. It seems that, the disagreement between the calculated and measured values is acceptable and realistic. Firstly, the computational model is “ideal” while the “sophisticated” factor, including the smooth of solid wall, conjugate between the test section and

manufacture accuracy of the real experimental model, are not considered. Secondly, the difference between the calculated mixing flow fields and real mixing flow fields also contributes the disagreement between the calculated and measured pumping ratio values. Generally, the present computational procedure for predicting the pumping ratio of mixer-ejector is satisfactory.

3.2 Parameter effects on performances

Fig. 7 shows the calculated temperature radial distributions at the mixing duct exit for the case of the area ratio 3.3 and the length-to-diameter ratio 0.8-2.5. As the length-to-diameter ratio increases with the area ratio being constant, the maximum temperature at the centerline of the mixing duct decreases and the minimum temperature near the wall increases. The uniformity of the temperature radial distribution also reflects the mixing efficiency of the mixer-ejector.

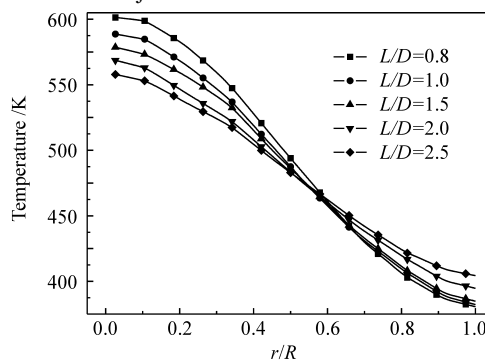


Fig. 7 Temperature radial distributions at mixing duct exit (varying length)

In order to evaluate the thermal mixing state quantitatively, the thermal mixing efficiency is defined as

$$\eta = \frac{\int T^{0.5} dm - T_p^{0.5} m_p - T_s^{0.5} m_s}{T_{mix}^{0.5} (m_p + m_s) - T_p^{0.5} m_p - T_s^{0.5} m_s} \quad (5)$$

where T is the static temperature and T_{mix} is the temperature of fully mixed flow.

The thermal mixing efficiencies along the mixing length in the case of $\lambda = 3.3$ and $L/D = 1$ are shown in Fig. 8. As x/L increases, the thermal mixing efficiency increases rapidly, showing that the thermal mixing efficiency is increasing. It is obvious that the streamwise vortices have an im-

portant role on enhancing rapidly mixing the primary and secondary flow together and reducing the core temperature of primary flow.

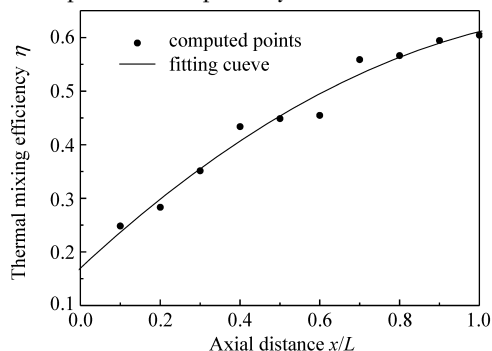
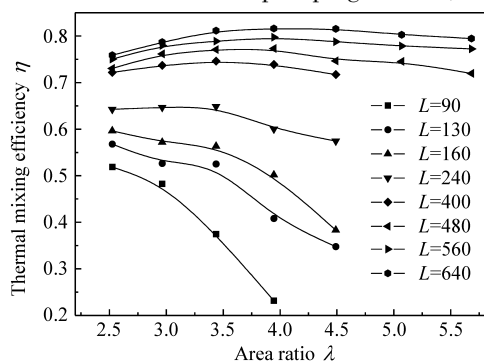
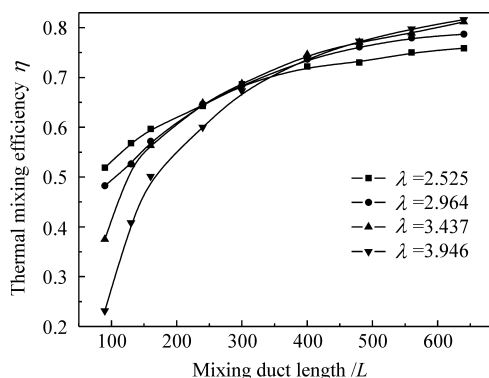


Fig.8 Thermal mixing efficiency *vs* axial distance

Fig. 9 shows the variation of the thermal mixing efficiencies at the mixing duct exit for different mixing duct lengths and area ratios, respectively. It is shown from Fig. 9(a) that the thermal mixing efficiency increases along with the increased length of the mixing duct for a giving value of mixing duct area ratio, which indicates that the increase of mixing duct length have a benefit to enhance the thermal mixing efficiency. This mixing characteristic is continent with the pumping feature, and for



(a) Thermal mixing efficiency *vs* area ratio



(b) Thermal mixing efficiency *vs* mixing duct length

Fig.9 Thermal mixing efficiency at the mixing duct exit

a giving mixing duct area ratio, the improvement of mixing efficiency is corresponding to the enhancement of pumping capacity.

For a giving value of mixing duct length, the relationship of thermal mixing efficiency *vs* mixing duct area ratio is more complicated than the former Fig. 9 (b). On the cases of short mixing duct length, the increase of area ratio (*i. e.*, the increase of the mixing duct diameter) induces the reduction of the thermal mixing efficiency. On the cases of long mixing duct length, the increase of area ratio causes the updown process of the thermal mixing efficiency. As known that the pumping capacity is associated with both mixing efficiency and secondary flow area, so the mixing characteristic is not continent with the pumping feature in the case of varying mixing duct area ratio.

A series of computations for determining the effects of area ratio and length-to-diameter ratio on the pumping capacity are shown in Fig. 10. It is seen that there is a peak pumping ratio value to correspond one λ for a giving mixing duct length and the λ corresponding to the peak pumping ratio increases as the mixing duct length increases. This feature is continent to the research by Skebe *et al*^[15], which indicates that there is an optimum performance design for the particular mixer-ejector system.

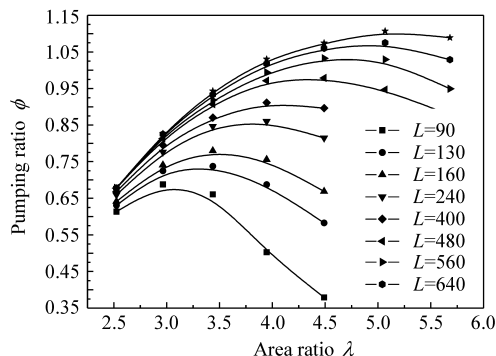


Fig. 10 Effects of mixing duct parameter on pumping ratio

4 Conclusions

Numerical computation and validation of the flow fields and pumping performances for the lobed mixer-ejector are conducted using full Navier-

Stokes equations. In the computation, the inlet of the primary flow uses the velocity boundary condition, and the inlet of the second flow and the outlet of the mixing flow use the pressure boundary condition. Compared with the relative experimental results, it is shown that the present calculation is satisfactory for predicting pumping capacity of mixer ejector.

The mixer ejector performances with variation of the area ratio and length to diameter ratio of the mixing duct are also demonstrated.

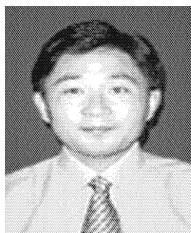
References

- [1] Presz W M, Reynolds G, McCormick D C. Thrust augment using mixer ejector diffuser systems[R]. AIAA Paper 94-0020, 1994.
- [2] Presz W M. Mixer/ ejector noise suppressors[R]. AIAA Paper 91-2243, 1991.
- [3] 张靖周, 李立国, 高潮, 等. 波瓣喷管红外抑制系统的实验研究[J]. 航空动力学报, 1997, 12(2): 212- 214.
Zhang J Z, Li L G, Gao C, *et al.* Experimental study on lobed nozzle IR suppression[J]. Journal of Aero Power, 1997, 12(2): 212- 214. (in Chinese)
- [4] Presz W M, Gousy R G, Morin B L. Forced mixer lobes in ejector designs[R]. AIAA Paper 86-1614, 1986.
- [5] DeBonis J R. Full navier stokes analysis of a two-dimensional mixer/ ejector nozzle for noise suppression[R]. AIAA Paper 92-3570, 1992.
- [6] Malecki R, Lord W. Navier stokes analysis of a lobed mixer and nozzle[R]. AIAA Paper 90-0453, 1990.
- [7] Koutmos P, McGuirk J J. CFD predictions of lobed mixer performance. Computer Methods in Applied Mechanics and Engineering[J]. 1995, 122: 131- 144.
- [8] Salman H, McGnirk J J, Page G J. A numerical study of vortex interactions in lobed mixer flow fields[R]. AIAA Paper 99-3409, 1999.
- [9] Ooba Y, Kodama H, Nakamura Y. Large eddy simulation analysis of a 18-lobe convoluted mixer nozzle[R]. AIAA Paper 2002-0717, 2002.
- [10] Liu Y H. Experimental and numerical investigation of circularly lobed nozzle with/ without central plug[J]. International

Journal of Heat and Mass Transfer, 2002, 45: 2577- 2585.

- [11] Zhang J Z, Xie Z R. Three dimensional computational study for flow fields within forced lobe mixer[R]. ISABE Paper 2003-1104, 2003.
- [12] Presz W M, Morin B L, Blinn R F. Short efficient ejector systems[R]. AIAA Paper 87-1837, 1987.
- [13] 张靖周, 单勇. 二维引射-混合器流场的数值研究与验证[J]. 航空动力学报, 2002, 17(5): 524- 527.
Zhang J Z, Shan Y. Numerical study and examination of 2D mixer ejector[J]. Journal of Aero Power, 2002, 17(5): 524- 527. (in Chinese)
- [14] Yakhot V, Smith L M. The renormalization group, the expansion and derivation of turbulence model[J]. Journal of Scientific Computing, 1972, 7(1): 35- 62.
- [15] Skebe S A, McCormick D C, Presz W M. Parameter effects on mixer ejector pumping performance[R]. AIAA Paper 88-0188, 1988.

Biographies:



ZHANG Jing zhou Born in 1964, Professor, he received B. S. from Tsinghua University in 1986 and M. S. from Southeast University in 1989 and doctoral degree from Nanjing University of Aeronautics and Astronautics in 1992 respectively. He has done a lot of researches on mixer ejector and enhanced heat transfer, and published several scientific papers in various periodicals. E-mail: zhangjz@nuaa.edu.cn



SHAN Yong Born in 1978, Ph.D student, he received B. S. and M. S. from Nanjing University of Aeronautics and Astronautics. Now he is working for his doctoral degree. His research interests are infrared stealth. Tel: 025-84892200-2523. E-mail: nuaasy@tom.com



LI Li guo Born in 1935, Professor, he received B. S. from Huazhong University in 1952 and then became a teacher in Nanjing University of Aeronautics and Astronautics. He has done a lot of researches on mixer ejector and enhanced heat transfer, and published many scientific papers in various periodicals.